High speed imaging of biofilm removal from a dental implant model using ultrasonic cavitation

Vyas, Nina; Grewal, Meher ; Kuehne, Sarah; Sammons, Rachel; Walmsley, Damian

DOI:
10.1016/j.dental.2020.03.003

Document Version
Peer reviewed version

Citation for published version (Harvard):
Vyas, N, Grewal, M, Kuehne, S, Sammons, R & Walmsley, D 2020, 'High speed imaging of biofilm removal from a dental implant model using ultrasonic cavitation', *Dental Materials*, vol. 36, no. 6, pp. 733-743. https://doi.org/10.1016/j.dental.2020.03.003

High Speed Imaging of Biofilm Removal from a Dental Implant Model using Ultrasonic Cavitation

Nina Vyas[1], Meher Grewal[1], Sarah A. Kuehne[1], Rachel L. Sammons[1], A. Damien Walmsley[1]

1. School of Dentistry, College of Medical and Dental Sciences, University of Birmingham, Birmingham, UK

Corresponding author:

Professor Damien Walmsley

Telephone +44 (0) 121 466 5493 (Secretary)

Email a.d.walmsley@bham.ac.uk

The School of Dentistry, College of Medical and Dental Sciences

University of Birmingham

5 Mill Pool Way

Edgbaston, Birmingham

UK

Declarations of interest: none

Abstract

Objectives: Current instruments cannot clean in between dental implant threads and effectively remove biofilm from the rough implant surface without damaging it. Cavitation bubbles have the potential to disrupt biofilms. The aim of this study was to see how biofilms can be disrupted using non-contact cavitation from an ultrasonic scaler, imaged inside a restricted implant pocket model using high speed imaging.

Methods*: Streptococcus sanguinis* biofilm was grown for 7 days on dental implants. The implants were placed inside a custom made restricted pocket model and immersed inside a water tank. An ultrasonic scaler tip was placed 0.5 mm away from the implant surface and operated at medium power or high power for 2s. The biofilm removal process was imaged using a high speed camera operating at 500 fps. Image analysis was used to calculate the amount of biofilm removed from the high speed images. Scanning electron microscopy was done to visualise the implant surface after cleaning.

Results: Cavitation was able to remove biofilm from dental implants. More biofilm was removed at high power. Scanning electron microscopy showed that the implant surface was clean at the points where the cavitation was most intense. High speed imaging showed biofilm removal underneath implant threads, in areas next to the ultrasonic scaler tip.

Significance: A high speed imaging protocol has been developed to visualise and quantify biofilm removal from dental implants *in vitro*. Cavitation bubbles from dental ultrasonic scalers are able to successfully disrupt biofilm in between implant threads.

Keywords: implant debridement, ultrasonic cleaning, biofilm disruption, cavitation

1. Introduction

Millions of dental implants are fitted each year [1] and they require professional care to maintain the health of the perimplant tissues. Maintenance of dental implants is required to treat and prevent peri-implantitis and implant failure [2]. There is a high prevalence of peri-implant disease which is often associated with bacterial infection [3, 4] and with the number of dental implants increasing, it is imperative that the biofilm build-up around them is removed effectively.

There is uncertainty about which is the most effective treatment for peri-implantitis [5, 6]. Surfaces are modified to promote osseointegration of the implant in the bone [7], but the presence of biofilm and its accumulation around implants often leads to peri-implantitis and bone loss [1]. This can lead to the roughened surfaces becoming exposed to the oral environment, allowing further biofilm to accumulate. These surfaces can be easily damaged by manual curettes or ultrasonic scaler tips which are used for periodontal therapy on teeth [8-10]. Other techniques such as titanium or plastic scaler tips do not effectively clean these implants, because they cannot clean in between the implant grooves and on the micro rough surface [8, 11]. Therefore, research is being done into finding more effective implant debridement methods [10, 12, 13].

A novel technique that could be used to remove biofilm from implants without causing damage is the use of cavitation bubbles [14]. Acoustic cavitation is the growth and collapse of microbubbles when exposed to an ultrasonic field [15]. They can disrupt bacterial biofilm by collapsing and releasing shear forces through various cavitation phenomena such as micro jet impingement and microstreaming [16]. Cavitation occurs around ultrasonic scalers in the cooling water flowing over the vibrating tip [17] and it is being researched as a novel method of biofilm removal which could clean dental implants without causing damage. Due to the small size of cavitation bubbles, they may be able to reach under implant grooves, as well as clean rough surfaces at the microscopic level. They also do not lead to any detectable alteration of the implant surface [18] which could prevent increased biofilm (re)growth and could help in re-osseointegration after peri-implantitis.

In order to understand how cavitation is able to remove biofilm from dental implants, real time imaging of the cleaning process is required to visualise the bubble dynamics and cleaning patterns. A high speed camera has been used in previous studies to image cavitation bubbles around dental instruments [18-20]. It also has potential to be used as a

tool to evaluate biofilm disruption methods. However, there has been no detailed investigation involving imaging of biofilm disruption occurring in real time on dental implants in a more clinically accurate, confined space model.

Therefore there are two aims of this study:

1. To investigate if biofilm removal can be imaged in a novel way in real time from a dental implant model in a confined space *in vitro*
2. To understand how cavitation from an ultrasonic scaler removes biofilm from an implant in a restricted pocket model

Experiments were done using high speed imaging, scanning electron microscopy and image analysis, on *Strepotococcus sanguinis* biofilms, which is an early coloniser on dental implant surfaces.

2. Materials and Methods

2.1 Restricted pocket model

The implants used in this study were Xive S Plus D 4.5/L8-13 implants (supplied by Dentsply Friadent, Mannheim Germany (now Dentsply Sirona) with a surface resembling the 'Friadent plus' surface which is sand blasted and acid etched [21]. The implants have evenly spaced threads approximately 0.6 mm apart. A restricted pocket model was constructed (Figure *10*) using lab putty by creating an impression of the implant in a block of activated lab putty and removing it before waiting for the lab putty to set. A section of the model was removed using a scalpel to make a vertical cut for the viewing window. A plastic coverslip (Thermanox™, 24 x 30mm, Nunc, ThermoFisher) was attached to the putty model to seal and form the viewing window for high speed imaging.

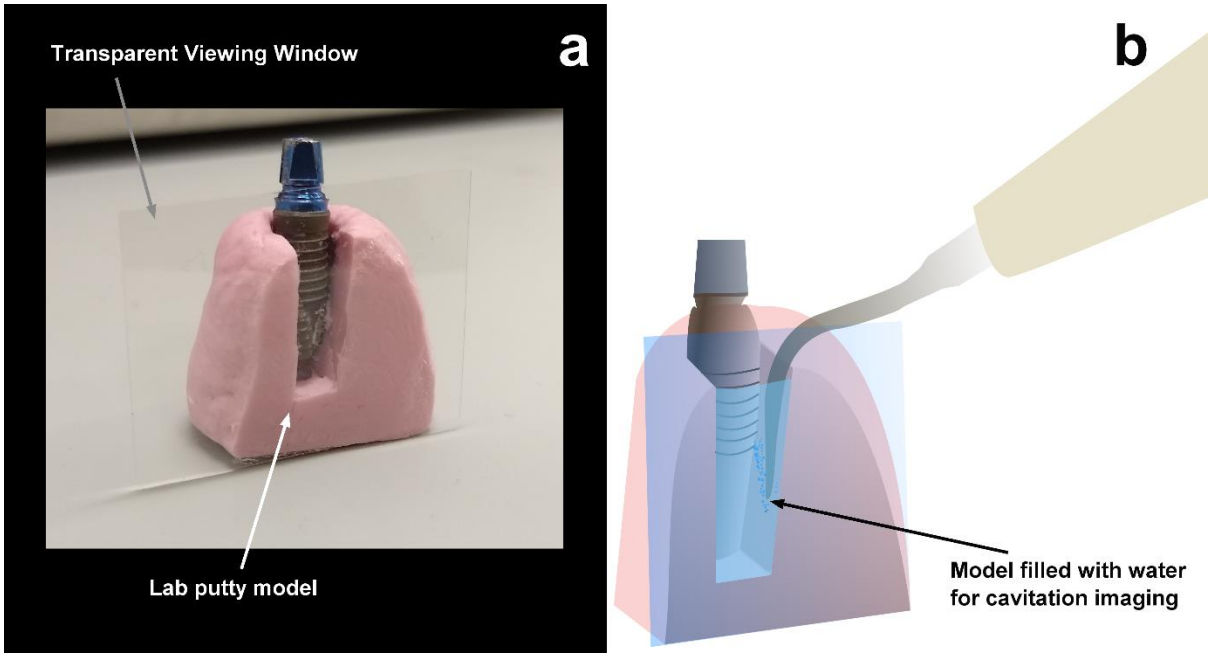

Figure 1 (a) Photograph of the restricted pocket model developed in this study to allow for high speed imaging of biofilm removal from a dental implant. (b) Schematic of the model in use for investigating cavitation from ultrasonic scalers

2.2 Biofilm Growth on Implants

The Gram-positive bacterium *Streptococcus sanguinis* (ATCC 10556) was used in the current study to form a simplistic early oral biofilm model for understanding the cavitation phenomena. Briefly, the stock microorganisms were recovered from porous storage beads maintained at −80 °C and initially grown on Tryptone Soya Agar (Oxoid, UK) media at 37 ˚C with 5% CO_2 for 3 days. 2-3 single colonies were used to inoculate 10 ml of Brain Heart Infusion (BHI) medium (Oxoid, U.K.) supplemented with 1% sucrose (Fluka Analytical, UK), which was incubated at 37 ˚C, shaking at 88 rpm overnight until it reached approximately 10^9 colony forming units/ml. This primary culture was serially diluted to 10^3 cfu/ml in BHI medium.

Artificial saliva was added to the biofilm culture surface to promote biofilm formation; this was prepared according to the method described by Pratten et al. [22], with the following chemicals from Sigma, UK (unless stated otherwise) added sequentially to RO (reverse osmosis) water : 0.35g/L sodium chloride (NaCl), 0.2g/L potassium chloride (KCL), 0.2g/L calcium chloride (CaCl2), 2g/L yeast extract, 1g/L lab lemco powder, 2.5g/L hog gastric

mucin and 5g/L proteose peptone. Reagents were mixed on a magnetic stir plate (Fisher scientific, Loughborough, UK) at ambient temperature for 1 hour. After autoclaving 1.25 mL of 40% sterile filtered urea (0.22 μm filter) was added to 1 L of the prepared artificial saliva. The prepared media was wrapped with aluminium foil to exclude light and prevent protein degradation [23] before being stored at 4 ±1 °C. 2 ml of the artificial saliva was pipetted into each well of a 24-well plate into which a sterile dental implant had been placed and was removed after 15 minutes, to condition the samples.

Two ml of the diluted *S. sanguinis* culture was added to each well of the 24-well plates. The 24-well plates were then incubated at 37 ˚C, 88 rpm for 168h to allow biofilm formation. The broth was replaced with 2 ml fresh BHI medium every 24 h. The dental implants were removed from the 24 well plates after a total of 7 days of incubation and then fixed in 0.1 M sodium cacodylate buffer and 2.5% glutaraldehyde (25% EM grade, Agar Scientific, Essex, UK). They were then stained with 0.1% Crystal Violet stain (Pro-Lab Diagnostics, UK) for 5 minutes and gently washed in Phosphate Buffered Saline (PBS) (Sigma-Aldrich, USA). Samples were stored in PBS at room temperature until high speed imaging to prevent dehydration.

2.3 High speed imaging

High speed imaging was used to image biofilm removal from the different surfaces via cavitation (Figure *11*). The implant was placed inside the restricted pocket model which was fixed vertically in a custom-made glass water tank filled with 180 ml reverse osmosis (RO) water. A P5 Newtron XS scaler (Satelec, Acteon, France) was used in conjunction with Tip 10P. The tip was immersed in the glass water tank and its position was fixed at 0.5 mm away from the implant by attaching it to a XYZ translation stage (PT3, Thorlabs Inc, NJ, USA) and a high-precision rotation mount (PRO1/M, Thorlabs Inc, NJ, USA). The axial rotation of the scaler tip was also maintained during each experiment. The sample was illuminated using an LED cold light source (Hayashi HDF7010, Japan) in reflectance mode. The biofilm removal was imaged using a high speed camera (Fastcam mini AX200, Photron, Japan). A long distance microscope zoom lens was attached to the camera (12x zoom lens system, Navitar, USA) with a 2x adapter. The scaler tip was operated at medium power (power 10) or high

power (power 20) for 2s. Five samples were imaged for each test condition. High speed imaging was done at 500 frames per second (fps), with a shutter speed of 1/1000 s, at a magnification of x0.8 or x4 giving a resolution of 12.5 µm/pixel or 2.5 µm/pixel respectively.

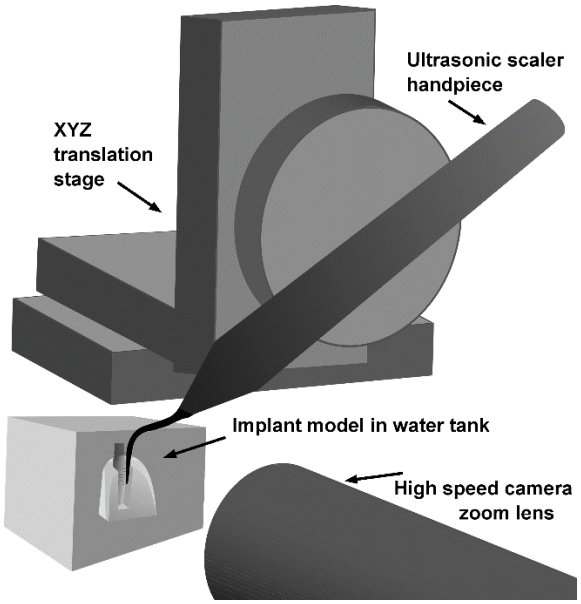

Figure 2 Schematic of the high speed imaging setup

2.4 Image Analysis

The biofilm removal on the implants was quantfied by calculating the area of biofilm on the implants from the high speed images. A high speed image taken before the scaler was operated was compared to a high speed image taken after operating the scaler tip for 2s. The two images were cropped to a rectangle which showed an identical area before and after cleaning. Fiji [24] (ImageJ, U.S. National Institutes of Health, Bethesda, Maryland, USA) was used to segment the images to calculate the area of biofilm on the implant surface before and after cleaning. Image segmentation was done using manual thresholding (**Error! Reference source not found.**). The number of white pixels in the thresholded image corresponded to the biofilm area. The ratio of pixels in the before and after thresholded images was taken to calculate the percentage of biofilm remaining on the surface. This was done for 5 repeat experiments for each power setting investigated and the mean value was plotted using Sigmaplot. Statistical significance was tested in Sigmaplot

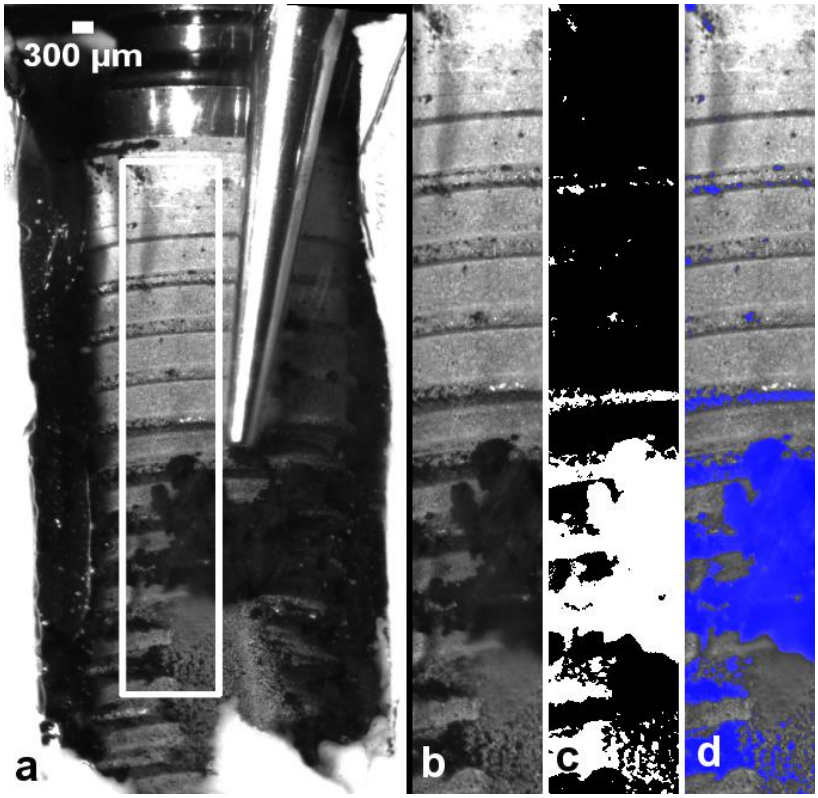

Figure 3 Image analysis steps on an example high speed image showing how the image was cropped (b) and thresholded (c). The blue overlay (d) of the thresholded image on the original image demonstrates the accuracy of the image segmentation

2.5 Scanning Electron Microscopy

Scanning electron microscopy (SEM) was used to image the implants at high magnification before biofilm growth and after the biofilm disruption experiments using an EVO MA-10 (Zeiss, Germany). Images were taken at x2000 and x5000 magnification, at a working distance of 11 mm and 10 kV. Samples were dehydrated using serial ethanol gradient immersions and then gold sputter-coated (Emitech K550X, Kent, UK) for SEM as previously described [25]. For imaging after cleaning, images were taken at the point where the tip of the ultrasonic scaler tip was closest to the implant (between the 5th and 6th threads, counted from the top) and also towards the top of the implant between the 1st and 2nd threads.

3. Results

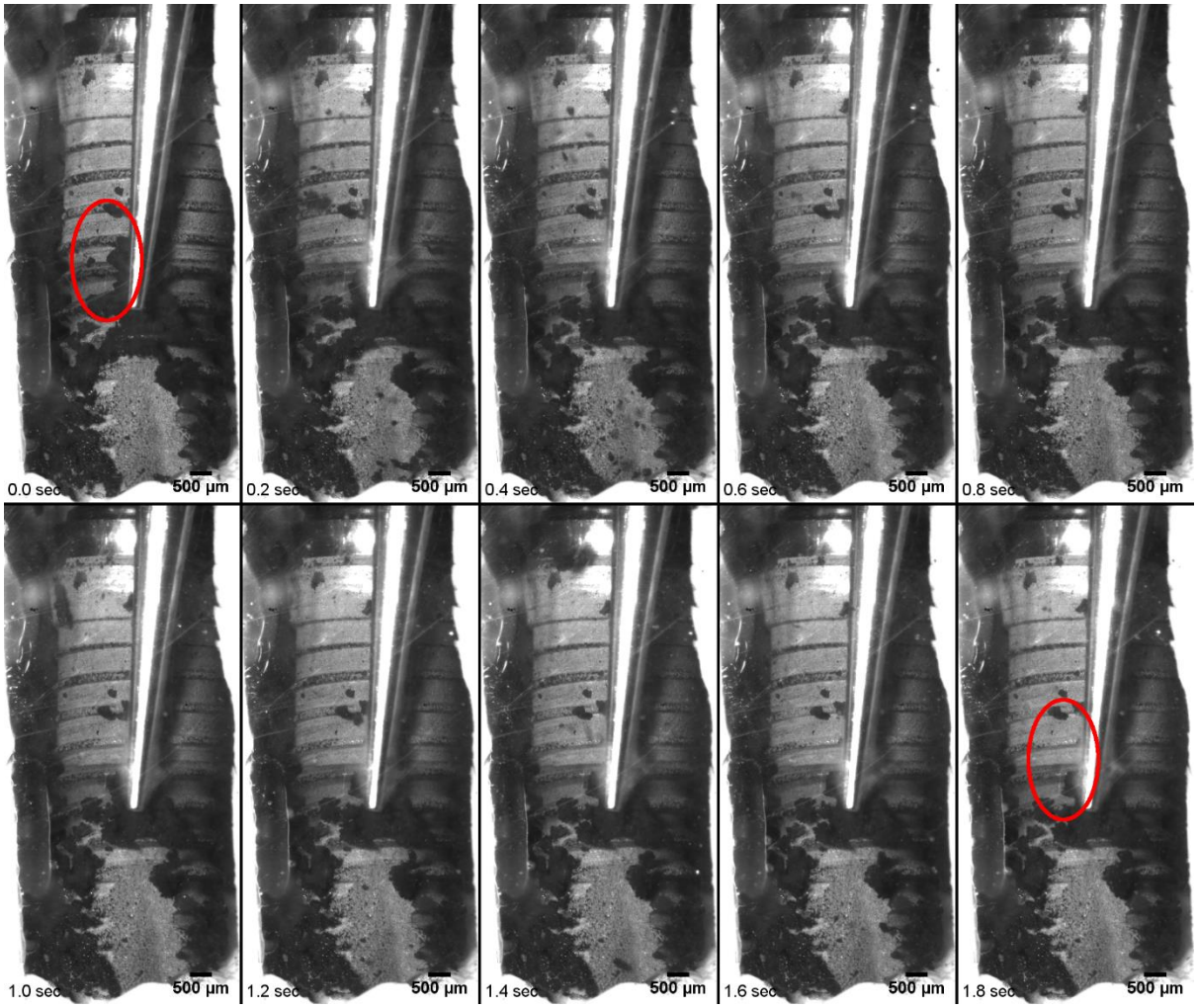

Figure 4 High speed image stills from cavitation applied at medium power, the red circles show areas of biofilm disruption.

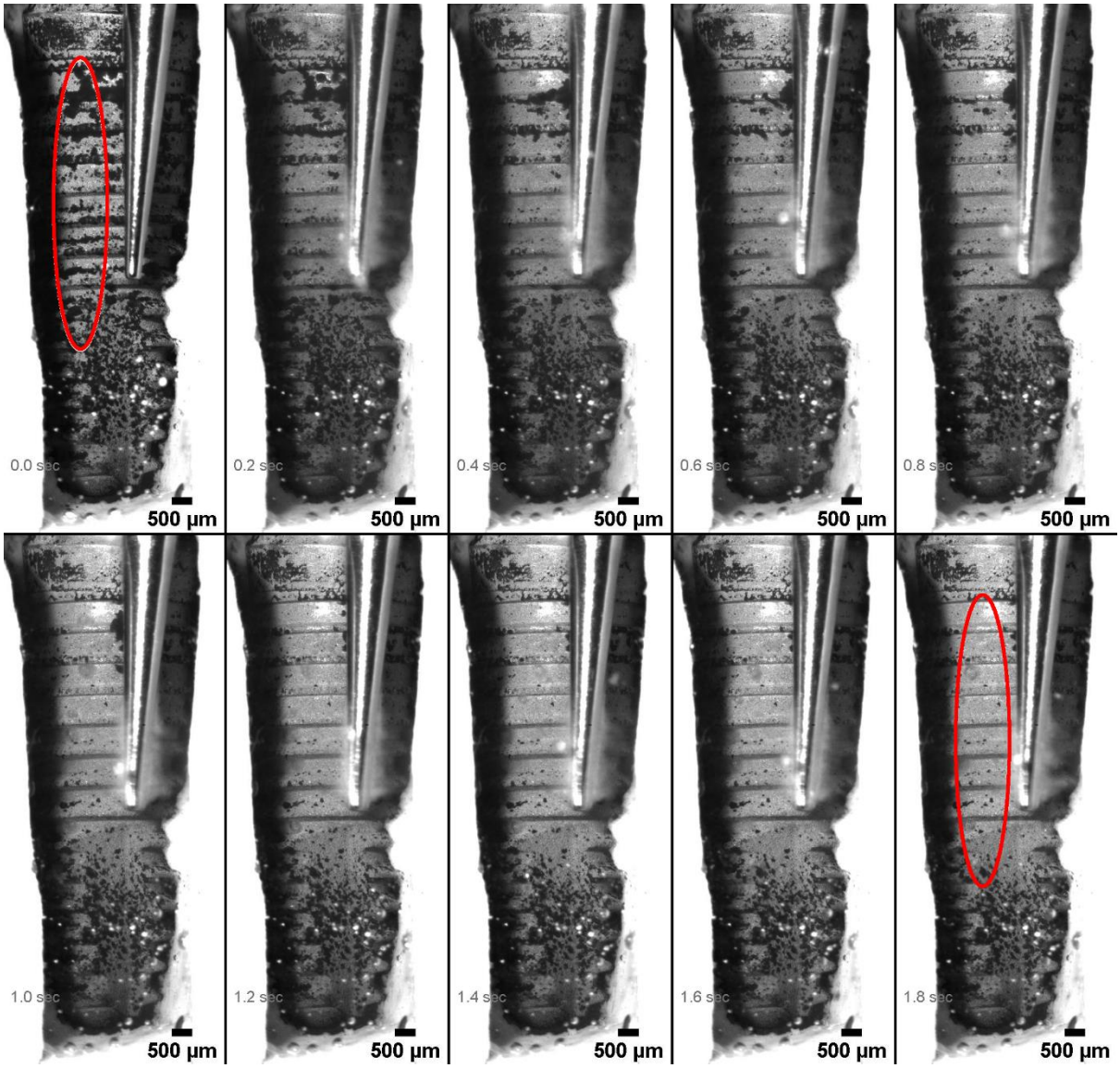

Figure 5 High speed image still from cavitation applied at maximum power, the red circles show areas of biofilm disruption.

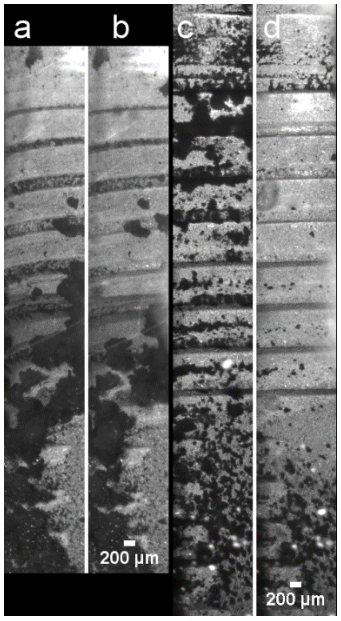

Figure 6 (a, b) implant before and after cleaning at medium power for 2 s. (c, d) implant after cleaning at high power for 2 s

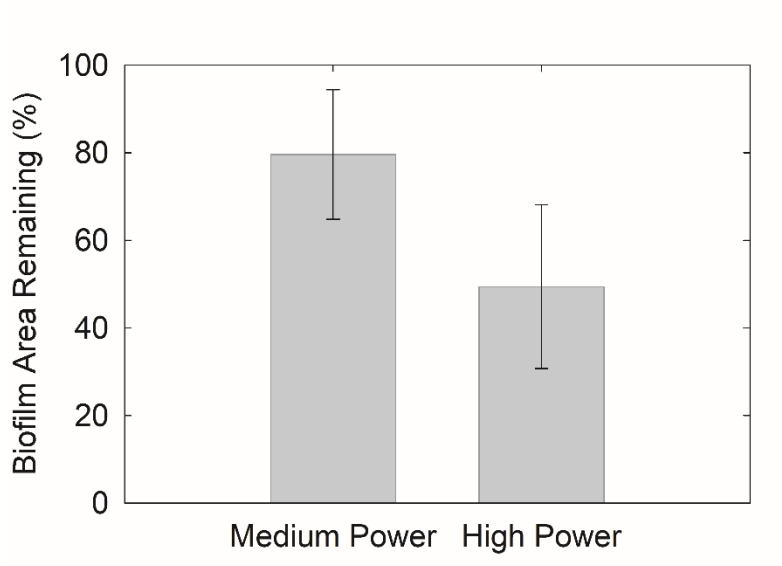

Figure 7 Biofilm surface area remaining on dental implants after 2s treatment with cavitation from an ultrasonic scaler n =5, $p<0.02$ (t-test)

Biofilm was removed from parts of the dental implants using cavitation from an ultrasonic scaler (Figure *13*, Figure *14*). High speed imaging showed that the majority of biofilm disruption occurred in the first 0.5 s (Figure *13*, Figure *14*). Cavitation bubbles were inertial, causing chaotic oscillations where the bubble collapsed and reformed continuously. Biofilm was removed from the implant threads by these oscillating cavitation bubbles (Figure *17*). At

power 10 small cavitation bubbles between 20-50µm in diameter appeared to be seen on the implant surface (supplementary video). Larger bubble clusters were also seen with diameters between 100-200 µm. At maximum power these bubble clusters were larger, with diameters between 200-500µm (Figure *17*). The implant grooves were evenly spaced, but bacterial biofilm formed irregularly on the implants, either in between the grooves or on raised surfaces. In some cases the biofilm formed in clusters with loosely attached biofilm streamers, whereas in other cases it formed in thin, long strips running parallel to the implant threads (supplementary videos). Both types of biofilm were removed via cavitation, although only in certain locations on the implant.

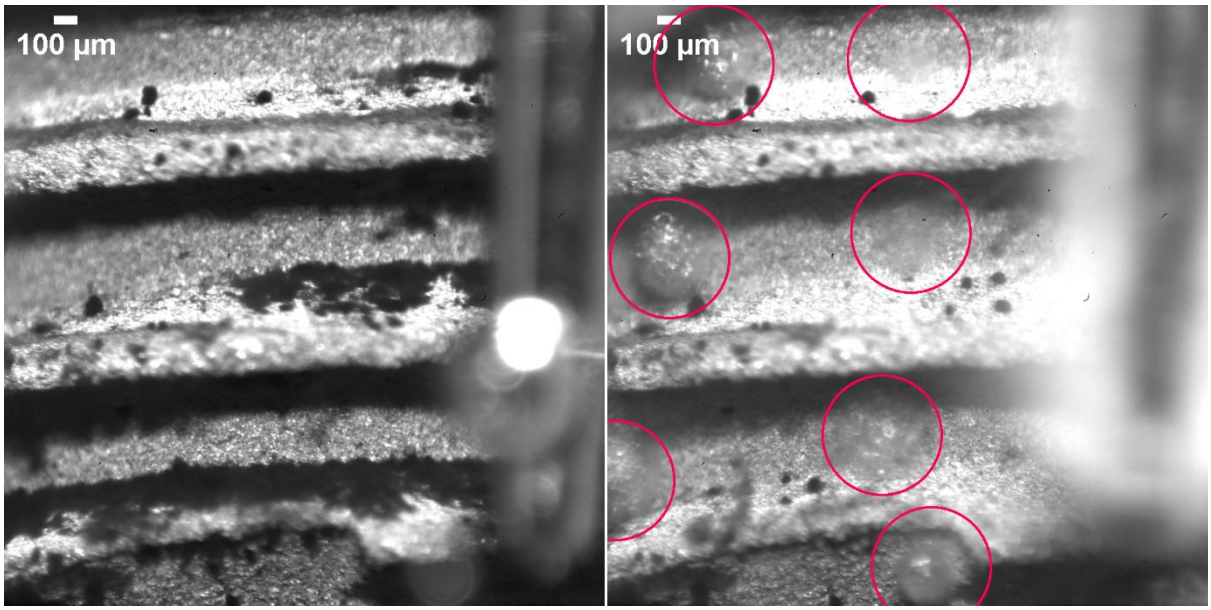

Figure 8 Stills from a high speed video showing a close up of the implant threads with stained biofilms (black) (left). (right) after 0.5 s most of the biofilm is removed. Cavitation bubble clusters can be seen in between the implant threads, circled in red. See supplementary video

At high power, the cavitation bubbles were active in a larger area around the tip, both parallel and perpendicular to the tip, therefore more biofilm was removed when the tip was operated at high power compared to medium power (Figure 15, Figure *16*). At both power settings, most of the biofilm at the apex of the implant, vertically below the free end of the scaler tip, was not removed (Figure *13*, Figure *14*). At both power settings biofilm was removed perpendicular to the tip, and mainly towards the free end of the tip. At high

power, some biofilm was also removed towards the implant abutment, which did not happen at medium power (supplementary videos).

At high power the diameter of the cavitation bubbles was similar to the width of the implant threads (Figure *17*). The bubbles travelled horizontally inside the threads and caused most of the biofilm disruption. Biofilm streamers, which are loosely attached parts at the top of a biofilm cluster, were removed first. In some cases smaller biofilm structures which were closer to the implant surface were not removed even after the cavitation bubble clusters made contact with them multiple times. This was seen at both medium and high power.

Scanning electron microscopy images showed that the implant surface was returned to its original condition at locations where the free end of the ultrasonic scaler tip was closest to the implant (Figure *18*). This was the case when cavitation was used at both medium and high power. However small clusters of biofilm were found still attached to the implant surface towards the top of the implant, for both power settings, although more biofilm remained when medium power was used.

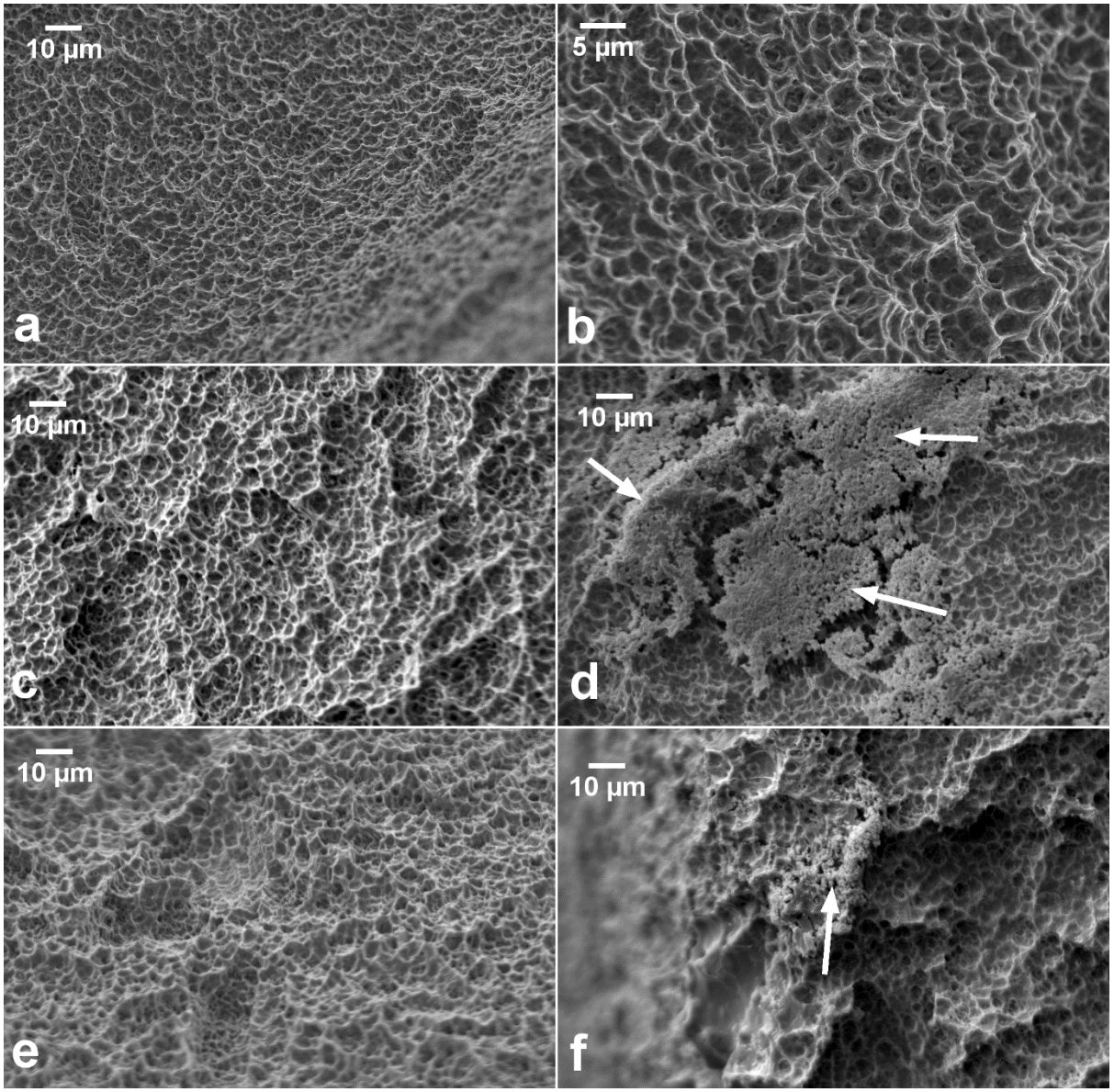

Figure 9 (a, b) The clean Friadent dental implant surface, before bacterial colonisation. (c) The implant surface closest to the free end of the ultrasonic scaler tip, after biofilm disruption using cavitation at medium power. (d) The implant surface towards the upper part of the dental implant after using cavitation at medium power, showing some biofilm clusters still attached (white arrows) (e) The implant surface closest to the free end of the ultrasonic scaler tip, after biofilm disruption using cavitation at high power. (f) The implant surface towards the upper part of the dental implant after using cavitation at high power, showing some biofilm clusters still attached (white arrow)

4. Discussion

The aim of this study was to develop a novel high speed imaging protocol to investigate dental implant debridement using ultrasonic cavitation. The cavitation occurring around an

ultrasonic scaler is thought to occur inside a periodontal pocket or around an implant pocket, but its effect has not been imaged before. Therefore, this study demonstrates how this process could be occurring *in vivo* using currently available instruments. We have developed a novel imaging protocol and demonstrated how bacterial biofilm is removed from an implant model in a confined space, which has not been reported before.

High speed videos showed that cavitation bubble clusters and small individual bubbles oscillating on the implant surface were able to clean biofilm that was in between the implant threads. This is difficult to achieve using currently available instruments such as ultrasonic scaler tips made specifically for implants, air polishing, and rotating brushes, so cavitation may be a more effective technique.

Image analysis showed that more biofilm was removed at high power (Figure *16*). At high power the area of low acoustic pressure around the tip would be larger. This would enable the cavitation to be powerful enough at further distances which are not possible at medium power. High speed images showed that at high power the larger cavitation bubbles cleaned more of the biofilm between the implant threads (Figure *17*). SEM images showed that the implant surface was completely intact, after cavitation at both power settings (Figure *18*). SEM images also showed effective biofilm removal at both power settings (Figure *18*). This suggests that small cavitation bubbles are just as effective at removing biofilm, but the larger bubbles moved quicker across the implant surface so could clean a bigger area in the same time span. This demonstrates that the power of the instrument is a major factor that affects biofilm removal. The instrument power is positively correlated with the vibration displacement of the ultrasonic scaler tip [18, 26]. As it is difficult for a clinician to hold the tip 0.5 mm away from the implant without making contact, this method is difficult to put into practise clinically because if the ultrasonic scaler tip contacts the implant it scratches the surface, which will increase biofilm accumulation and may cause problems with re-osseointegration [27], but further research can be done to enable ultrasonic scalers to be used in a non-contact mode.

Only some parts of the dental implant were cleaned. This shows that the cavitation bubbles were effective but only in a limited area. This is likely to be because the cavitation bubbles are active in only a small area around the tip where the acoustic pressure is low enough for cavitation to occur. Since a large amount of biofilm on the implant was not disrupted, the

scaler should be moved every 0.5 s to ensure cleaning is more effective and biofilm is removed from all areas of the implant during clinical use. In addition, it is important to prioritise moving the scaler vertically within a pocket, as cavitation occurs perpendicular to the implant tip. This has also been advised previously for using air polishing devices as they also only clean a localised area [28].

Most of the cleaning happened in the first 0.5 s of operating the scaler tip. Holding the scaler in the same position for longer did not significantly increase the biofilm removal. This suggests that some biofilm clusters have a larger attachment force. High speed videos showed cavitation bubbles crossing over some biofilm structures without disrupting them, so it is likely that bubbles with more force are needed to remove these types of biofilm. This could be achieved by holding the tip closer to the implant or at a higher power.

Previous work has shown that the most cavitation occurs near the free end of the ultrasonic scaler tip [18]. In these experiments this part of the tip was positioned in the same location for each experiment, between the 5th and 6th implant threads. Scanning electron microscopy showed that the biofilm was completely removed at the point where there was more cavitation (between the 5th and 6th implant threads) but there were small clusters of biofilm remaining at other points along the implant such as on the first two threads, this was also seen in high speed imaging. This demonstrates that the cavitation is effective at removing biofilm at the microscopic level but only in localised areas close to the free end of the ultrasonic scaler tip. This was observed both at power 10 and at power 20, but there was a greater amount of cleaning at power 20 towards the top of the implant, compared to power 10. This is similar to what was seen in the lower magnification high speed images, showing that the cavitation bubbles are not powerful enough at increasing distances away from the tip at medium power.

Previous work has investigated the cleaning effectiveness of other dental implant decontamination methods such air polishing, lasers, manual curettes or ultrasonic scaler tips in contact with the implant [8, 9, 12, 28-30]. The latter two cause scratches on the implant surface which can promote more biofilm formation. Air polishing did not cause implant surface damage but it did leave some glycine residue on the implants when viewed under SEM [8], as did the use of titanium curettes [9, 10], which may be problematic during re-osseointegration [27]. The current study and a previous study showed, using SEM, that

ultrasonic cavitation did not damage the implant surface (Figure *18*). In addition, because only water was used, there was no residue left on the implants. Many previous studies *in vitro* were done using an artificial biofilm such as ink or a calcium phosphate coating [8, 12, 28-30], but this is not clinically accurate as ink and biofilm have different attachment and viscoelastic properties. Lasers were investigated using bacterial biofilm but they did not physically disrupt the biofilm, although they had an antimicrobial effect [27]. Another limitation of many of these studies is that the image analysis procedures used for calculating the amount of biofilm removed were not fully explained [8, 12, 28-30]. This does not allow accurate reproduction of the method and may increase bias in reporting of the results.

There are several advantages of using this high speed imaging protocol compared to methods used in previous studies when assessing implant cleaning. Previous studies on the effectiveness of cleaning dental implants have used photographic studies to rate the cleaning potential *in vitro*. In one study photographs were stitched together to obtain higher magnification images of the implant [30]. The use of high speed imaging combined with a zoom lens allows the cleaning and evaluation to be done in one experiment. In addition the high speed video shows in real time the cleaning mechanism including where it occurs first. This will help in improving the use and further design of ultrasonic dental instruments. Cleaning happens over very fast timescales (under 1s) and more research about the disruption process is required to evaluate the initial cleaning. In addition the use of a zoom lens helps to image removal at sub-millimetre resolution where the magnification is lower than SEM so the whole implant can be imaged. It is higher magnification than regular photography which was used in previous studies, therefore the biofilm and the cavitation bubbles can be visualised more effectively.

The restricted pocket model developed in this study for high speed imaging makes the experiment clinically relevant whilst still being able to image the cleaning process. It is cost-effective and easy to construct and could be used in other similar studies. It can also be easily adapted to investigate other periodontal therapy methods and also other geometries such as interproximal spaces or root furcations.

A limitation of the study is that the tip was immersed in a water tank, whereas clinically cavitation happens in the cooling water flowing over the ultrasonic scaler tip. This was done to image the process with high speed imaging but it might also simulate a clinical situation

such as inside a pocket where cooling water from the tip may accumulate. However this may not occur in all clinical situations. Nevertheless, the information gained from high speed imaging will allow optimisation of the tip to be used clinically in a non-touch mode. In this study the imaging protocol has been developed and tested on cavitation, but it was not compared with other methods because it was out of the scope of this study. Further research is required to compare this removal process alongside other implant decontamination methods such as air polishing, implant specific scaler tips and rotating brushes. Further work can also be done using cavitation generated from different shaped scaler tips and on different types of dental implants to see how the different geometries affect the cavitation bubble movements on the surface. In the current study we chose to image a single species biofilm because we wished to test our imaging protocol and ensure that changes in the results were not due to different bacteria in the biofilm, however this protocol can be used to test removal on more clinically realistic, multi-species peri-implant biofilms. It would also be interesting to investigate if multi-species biofilms have different attachment forces on implants and how this affects their removal with different methods.

The high speed imaging method developed in this study is not able to quantify the whole biofilm on the dental implant because it is a complex 3D structure. Therefore further imaging methods using micro computed tomography could be developed to image biofilm in 3D. These methods, once developed, could be used in conjunction with the high speed imaging method developed in this study. This will allow researchers to visualise how the biofilm is removed and also show the biofilm distribution across the implant in 3D before and after cleaning. The methods used in the current study image the same area before and after cleaning, therefore it is an accurate representation of the cleaning ability of the instrument in the area tested. We believe that the novel methods developed in this study will allow all of these to be studied in more detail than before.

5. Conclusion

In conclusion this study demonstrates that cavitation removes biofilm from in between implant threads, which is difficult to do using currently available methods. Cavitation at high power from an ultrasonic scaler tip is able to clean more biofilm from dental implants within

2 s compared to cavitation at medium power. Further development of this method could allow the tip to be used in a non-contact mode at high power to clean dental implants using only cavitation.

Acknowledgements

This work was supported by the Engineering and Physical Sciences Research Council (EPSRC) (EP/P015743/1)

References

[1] Klinge B, Hultin M, Berglundh T. Peri-implantitis. Dental Clinics. 2005;49:661-76.
[2] Chen S, Darby I. Dental implants: Maintenance, care and treatment of peri-implant infection. Aust Dent J. 2003;48:212-20.
[3] Derks J, Tomasi C. Peri-implant health and disease. A systematic review of current epidemiology. J Clin Periodontol. 2015;42:S158-S71.
[4] Jung RE, Pjetursson BE, Glauser R, Zembic A, Zwahlen M, Lang NP. A systematic review of the 5-year survival and complication rates of implant-supported single crowns. Clinical oral implants research. 2008;19:119-30.
[5] Esposito M, Grusovin MG, Worthington HV. Interventions for replacing missing teeth: treatment of peri-implantitis. Cochrane database of systematic reviews. 2012.
[6] Kotsovilis S, Karoussis IK, Trianti M, Fourmousis I. Therapy of peri-implantitis: a systematic review. J Clin Periodontol. 2008;35:621-9.
[7] Le Guéhennec L, Soueidan A, Layrolle P, Amouriq Y. Surface treatments of titanium dental implants for rapid osseointegration. Dent Mater. 2007;23:844-54.
[8] Keim D, Nickles K, Dannewitz B, Ratka C, Eickholz P, Petsos H. In vitro efficacy of three different implant surface decontamination methods in three different defect configurations. Clinical oral implants research. 2019;30:550-8.
[9] Schmidt KE, Auschill TM, Heumann C, Frankenberger R, Eick S, Sculean A, et al. Influence of different instrumentation modalities on the surface characteristics and biofilm formation on dental implant neck, in vitro. Clinical oral implants research. 2017;28:483-90.
[10] Louropoulou A, Slot DE, Van der Weijden FA. Titanium surface alterations following the use of different mechanical instruments: a systematic review. Clinical Oral Implants Research. 2012;23:643-58.
[11] Mann M, Parmar D, Walmsley AD, Lea SC. Effect of plastic-covered ultrasonic scalers on titanium implant surfaces. Clinical Oral Implants Research. 2012;23:76-82.
[12] Sahrmann P, Ronay V, Hofer D, Attin T, Jung RE, Schmidlin PR. In vitro cleaning potential of three different implant debridement methods. Clinical Oral Implants Research. 2013.
[13] Ioannidis A, Thurnheer T, Hofer D, Sahrmann P, Guggenheim B, Schmidlin PR. Mechanical and hydrodynamic homecare devices to clean rough implant surfaces–an in vitro polyspecies biofilm study. Clinical oral implants research. 2015;26:523-8.
[14] Vyas N, Sammons RL, Addison O, Dehghani H, Walmsley AD. A quantitative method to measure biofilm removal efficiency from complex biomaterial surfaces using SEM and image analysis. Sci Rep. 2016;6:32694.
[15] Brennen CE. Cavitation and Bubble Dynamics: Cambridge University Press; 2013.

[16] Verhaagen B, Rivas DF. Measuring cavitation and its cleaning effect. Ultrason Sonochem. 2016;29:619-28.
[17] Lea SC, Price GJ, Walmsley AD. A study to determine whether cavitation occurs around dental ultrasonic scaling instruments. Ultrason Sonochem. 2005;12:233–6.
[18] Vyas N, Pecheva E, Dehghani H, Sammons RL, Wang QX, Leppinen DM, et al. High Speed Imaging of Cavitation around Dental Ultrasonic Scaler Tips. PLoS One. 2016;11:e0149804.
[19] Macedo RG, Verhaagen B, Fernandez Rivas D, Gardeniers JGE, van der Sluis LWM, Wesselink PR, et al. Sonochemical and high-speed optical characterization of cavitation generated by an ultrasonically oscillating dental file in root canal models. Ultrason Sonochem. 2014;21:324-35.
[20] Blanken J, De Moor RJG, Meire M, Verdaasdonk R. Laser induced explosive vapor and cavitation resulting in effective irrigation of the root canal. Part 1: A visualization study. Lasers Surg Med. 2009;41:514-9.
[21] Rupp F, Scheideler L, Rehbein D, Axmann D, Geis-Gerstorfer J. Roughness induced dynamic changes of wettability of acid etched titanium implant modifications. Biomaterials. 2004;25:1429-38.
[22] Pratten J, Smith A, Wilson M. Response of single species biofilms and microcosm dental plaques to pulsing with chlorhexidine. Journal of Antimicrobial Chemotherapy. 1998;42:453-9.
[23] Lodovici M, Raimondi L, Guglielmi F, Gemignani S, Dolara P. Protection against ultraviolet B-induced oxidative DNA damage in rabbit corneal-derived cells (SIRC) by 4-coumaric acid. Toxicology. 2003;184:141-7.
[24] Schindelin J, Arganda-Carreras I, Frise E, Kaynig V, Longair M, Pietzsch T, et al. Fiji: an open-source platform for biological-image analysis. Nat Meth. 2012;9:676-82.
[25] Sammons RL, Lumbikanonda N, Gross M, Cantzler P. Comparison of osteoblast spreading on microstructured dental implant surfaces and cell behaviour in an explant model of osseointegration: a scanning electron microscopic study. Clinical oral implants research. 2005;16:657-66.
[26] Lea SC, Felver B, Landini G, Walmsley AD. Three-dimensional analyses of ultrasonic scaler oscillations. J Clin Periodontol. 2009;36:44-50.
[27] Al-Hashedi AA, Laurenti M, Benhamou V, Tamimi F. Decontamination of titanium implants using physical methods. Clinical oral implants research. 2017;28:1013-21.
[28] Tastepe CS, Lin X, Donnet M, Wismeijer D, Liu Y. Parameters that improve cleaning efficiency of subgingival air polishing on titanium implant surfaces: An in vitro study. Journal of periodontology. 2017;88:407-14.
[29] Sahrmann P, Ronay V, Sener B, Jung RE, Attin T, Schmidlin PR. Cleaning potential of glycine air-flow application in an in vitro peri-implantitis model. Clinical oral implants research. 2013;24:666-70.
[30] Wei MC, Tran C, Meredith N, Walsh LJ. Effectiveness of implant surface debridement using particle beams at differing air pressures. Clinical and experimental dental research. 2017;3:148-53.

Figure Legends:

Figure 10 (a) Photograph of the restricted pocket model developed in this study to allow for high speed imaging of biofilm removal from a dental implant. (b) Schematic of the model in use for investigating cavitation from ultrasonic scalers

Figure 11 Schematic of the high speed imaging setup

Figure 12 Image analysis steps on an example high speed image showing how the image was cropped (b) and thresholded (c). The blue overlay (d) of the thresholded image on the original image demonstrates the accuracy of the image segmentation

Figure 13 High speed image stills from cavitation applied at medium power, the red circles show areas of biofilm disruption.

Figure 14 High speed image still from cavitation applied at maximum power, the red circles show areas of biofilm disruption.

Figure 15 (a, b) implant before and after cleaning at medium power for 2 s. (c, d) implant after cleaning at high power for 2 s

Figure 16 Biofilm surface area remaining on dental implants after 2s treatment with cavitation from an ultrasonic scaler n =5, $p<0.02$ (t-test)

Figure 17 Stills from a high speed video showing a close up of the implant threads with stained biofilms (black) (left). (right) after 0.5 s most of the biofilm is removed. Cavitation bubble clusters can be seen in between the implant threads, circled in red. See supplementary video

Figure 18 (a, b) The clean Friadent dental implant surface, before bacterial colonisation. (c) The implant surface closest to the free end of the ultrasonic scaler tip, after biofilm disruption using cavitation at medium power. (d) The implant surface towards the upper part of the dental implant after using cavitation at medium power, showing some biofilm clusters still attached (white arrows) (e) The implant surface closest to the free end of the ultrasonic scaler tip, after biofilm disruption using cavitation at high power. (f) The implant surface towards the upper part of the dental implant after using cavitation at high power, showing some biofilm clusters still attached (white arrow)